Biophysical Journal, Volume *110*

Supplemental Information

The Influence of Ionic Environment and Histone Tails on Columnar Order of Nucleosome Core Particles

Nikolay V. Berezhnoy, Ying Liu, Abdollah Allahverdi, Renliang Yang, Chun-Jen Su, Chuan-Fa Liu, Nikolay Korolev, and Lars Nordenskiöld

Biophysical Journal

Supporting Material

The Influence of Ionic Environment and Histone Tails on Columnar Order of Nucleosome Core Particles

Nikolay V. Berezhnoy,[1] Ying Liu,[1] Abdollah Allahverdi,[1] Renliang Yang,[1] Chun-Jen Su,[2] Chuan-Fa Liu,[1] Nikolay Korolev,[1] and Lars Nordenskiöld[1,*]

[1]School of Biological Sciences, Nanyang Technological University, Singapore; and [2]National Synchrotron Radiation Research Center, Hsinchu, Taiwan

*Correspondence: larsnor@ntu.edu.sg

Supporting Materials and Methods

Preparation and purification of histones

Genes coding wild-type and modified *X. laevis* core histones H2A, H2B, H3 and H4 in the pET-3a plasmids were expressed using *E. coli* strain BL21 (DE3) pLysS. Gene constructs of mutated histones H4-K16Q, H4-QuadQ and H2A-STT were prepared from wild type genes using QuickChange site-directed mutagenesis kit (1). Gene constructs of tailless histones gH2A, gH2B, gH3 and gH4 were cloned from wild type genes using PCR (2, 3). Gene construct with H4 residues 20-102 and Lys20Cys mutation used in preparation of H4-K16Ac and H4-QuadAc was prepared from wild type gene using PCR (1).

Single colonies of *E. coli* transformed with histone constructs were grown in 2xTY medium containing appropriate antibiotics, the histone expression was induced by 0.4 mM isopropyl-β,D-thiogalactopyranoside (IPTG) at OD_{600} = 0.6. After 3 hours of incubation at 37˚C (WT) or 30˚C (modified histones) bacterial cells were harvested by centrifugation (7,000 g, 7 min, 25°C). The bacteria resuspended in 100 mL of wash buffer (1 M Tris·HCl, 100 mM NaCl and 1 mM β-mercaptoethanol) were lysed by flash freezing in liquid nitrogen and thawing. The cell suspension was sonicated until the loss of viscosity using SONICS Vibra-Cell ultrasonic processor at amplitude of 25% with two-second-pulse. The inclusion bodies containing histones were precipitated from the sonication mixture (12,000 g, 15 min, 4°C), and washed three times in 200 mL of wash buffer containing 1% (v/v) Triton X-100 by repeated resuspension and centrifugation, followed by washing twice with 200 mL wash buffer to remove the detergent. The histones from inclusion bodies were dissolved in 1 mL of dimethylsulfoxide (DMSO) at room temperature, followed by addition of 40 mL of S-200 unfolding buffer (7 M guanidinium·HCl, 20 mM Na-acetate at pH 5.2 and 10 mM dithiothreitol (DTT)).

The histones were purified at room temperature by gel-filtration and cation-exchange chromatography and the purity was checked by 18% SDS-PAGE. The histones were purified using HiPrep 26/60 Sephacryl S-200 HR gel-filtration column (GE Healthcare Life Sciences) in SAUDE-1000 buffer (7 M deionized urea, 20 mM Na-acetate at pH 5.2, 1000 mM NaCl, 5 mM β-mercaptoethanol and 1 mM EDTA). Purified histones were dialyzed against water containing 5 mM β-mercaptoethanol, using Spectra/Por dialysis tubing (MWCO 3,500 Da), centrifuged to remove aggregates (10,000 rpm, 10 min at 4 ˚C) and lyophilized.

The wild type histones were dissolved in SAUDE-200 buffer (7 M deionized urea, 20 mM Na-acetate at pH 5.2, 200 mM NaCl, 5 mM β-mercaptoethanol and 1 mM EDTA) and the modified histones were dissolved in SAUDE-0 buffer (7 M deionized urea, 20 mM Na-acetate at pH 5.2, 5 mM β-mercaptoethanol and 1 mM EDTA) and purified in a 15% - 40% gradient of SAUDE-1000 buffer using Resource S 6 mL cation exchange column (GE Healthcare Life Sciences).

Acetylated forms of the histone H4, H4K16Ac and H4-QuadAc (tetraacetylated form at the positions 5, 8, 12 and 16) were obtained by native chemical ligation (NCL) and S-alkylation reactions as described in earlier work (1, 4). Briefly NCL reaction was carried with 1CL reaction was cathioester and truncated histone H4(20-102)K20C in ligation buffer (6M GdnHCl, 0.2M phosphate, 20 mM TCEP, 1.5% benzyl mercaptan, pH 8.0). The ligation product was purified by semi-preparative HPLC. Next, the S-alkylation reaction was performed between the ligation product and 2-bromoethylamine dissolved in alkylation buffer (4M GdnHCl, 1M HEPES, 10mM D/L-methionine, 5mM TCEP, pH 7.8). The product was isolated either with C4 semi-preparative

HPLC or by dialysis against 2-mercaptoethanol-containing water. It was shown (4) that S-alkylated analog of lysine at position 20 of the histone H4 does not influence of biophysical and biochemical properties of the nucleosome arrays constructed with this form the of the H4 histone.

Histone octamer refolding and purification

Lyophilized core histone proteins H2A, H2B, H3 and H4 (WT or modified) were dissolved in HO-unfolding buffer (7 M guanidinium HCl, 10 mM Tris·HCl, pH 7.5 and 10 mM DDT). The concentration of each nucleosome histone or the mutants was determined by the absorbance at λ = 276 nm, with the molar extinction coefficients calculated from the amino acid composition (5). The histones were combined at molar ratio of H2A:H2B:H3:H4 = 1:1:1.2:1.2 and a final protein concentration of 1 mg/mL. The dialysis against HO-refolding buffer (2 M NaCl, 10 mM Tris·HCl at pH7.5, 1 mM EDTA and 5 mM beta-mercaptoethanol) was carried at room temperature using Spectra/Por dialysis membrane (MWCO 6-8 kDa). The HO solution was centrifuged (9,000 g, 10 min, 20°C), concentrated to 10 mg/mL using Amicon ultra centrifugal filter (MWCO 10 kDa) and purified using the HiPrep 26/60 Sephacryl S-200 HR gel filtration column in the HO-refolding buffer. The purity and completeness of the HO refolding was checked by 18% SDS-PAGE. The octamer solutions were stored in 50% glycerol at –20°C.

DNA preparation

The DNA used in this work to reconstitute nucleosome core particle was the 145 bp '601' Widom nucleosome-positioning sequence (6). In a few SAXS measurements, NCP reconstituted with the 147 bp palindromic human α-satellite DNA fragment (7, 8) was used.

The pUC19 plasmid containing eight copies of 145 bp '601' DNA flanked by EcoRV restriction enzyme recognition sites was a gift from the laboratory of Dr. Curt. A. Davey (Nanyang Technological University).

The pUC19 plasmid containing 145 bp DNA was amplified in *E. coli* HB101 and extracted by alkaline lysis method. The plasmid was purified by treated with RNase, phenol, and precipitated by PEG 6000. The plasmid was digested by EcoRV, and the 145 bp DNA was separated from the vector by PEG 6000 and extracted by chloroform: 3-methyl-1-butanol mixture (v/v = 24:1). The purity of 145 bp DNA was checked by 10% PAGE.

NCP reconstitution

The 145 bp DNA and HO were mixed in a range of molar ratios in a total volume of 200 µl, containing 6 µM (0.544 mg/mL) 145 bp DNA, 4-6 µM HO, 2 M KCl and 10 mM DTT. The mixture in a Spectra/Por dialysis membrane (MWCO 6-8 kDa) was dialyzed in buffer (20 mM Tris HCl pH 7.5, 1mM EDTA and 1mM DTT) with step-wise decrease of KCl concentration: 1.3 M, 0.85 M, 0.65 M, 0.45 M and 10 mM. The purity of NCP and the absence of free 145 bp DNA was checked on 5% PAGE. The optimal ratio was chosen for the large-scale preparation. The yield was comparable for all NCP types, wild type, mutated and with deleted tails. The presence of less than 5% of free DNA was tolerated in the NCP preparations used for precipitation by cations and solution measurements. The free DNA remained in the solution during NCP precipitation by Mg^{2+}. The presence of free DNA did not affect the scattering in H2A-STT sample, the scattering was comparable with WT-NCP and H4-K16Q.

Small angle X-ray scattering (SAXS)

The NCP aggregates at 8 mg/mL of the final NCP concentration in 20 mM Tris-HCl buffer (pH 7.5) were prepared by adding 40 μl of multivalent cation salt solution into 160 μL of 10 mg/mL NCP stock solution. The suspended NCP aggregates were transferred into the quartz capillary d = 1.5 - 2 mm (Charles Supper Company, USA), sealed with wax and centrifuged to precipitate aggregates.

Measurements were made with X-ray flux of 14.0 keV (λ= 0.886 Å) at the Beamline 23A SWAXS endstation of the National Synchrotron Radiation Research Center (Hsinchu, Taiwan) (9). The X-ray beam was directed at the center of the precipitate above the curved bottom of the capillary. Scattering profiles were recorded with charge-coupled device-based area detector (MarCCD165, Mar Evanston, IL, USA) at 1.75 m sample-to-detector distance. The scattering wave vector $q = 4\pi \cdot sin(\theta)/\lambda$ (2θ is the scattering angle) was calibrated with silver behenate. The two-dimensional diffraction pattern was circularly averaged into one-dimensional q versus I spectrum. The raw Bragg reflection data were corrected for background scattering and sample transmission before analyzed with the software OriginPro 9.

Table S1. Composition of the NCP samples studied by SAXS.

	NCP type	NCP concentration, mg/mL	Cation	Cation concentration, mM
1	WT-NCP	1.25 – 17	K^+	10 – 100
		8	Mg^{2+}	3 – 80
		8	$CoHex^{3+}$	1.2 – 30
		8	Spd^{3+}	3.88 – 11.64
		8	Spm^{4+}	1.45 – 5.82
2	H4-K16Q	8	Mg^{2+}	12 – 50
		8	$CoHex^{3+}$	0.8 – 5
3	H4-K16Ac	8	Mg^{2+}	5 – 50
		8	$CoHex^{3+}$	1.7 – 8
4	H4-QuadQ	8	Mg^{2+}	10 – 70
		8	$CoHex^{3+}$	0.8 – 3.7
5	H4-QuadAc	8	Mg^{2+}	10, 25
		8	$CoHex^{3+}$	4, 5
6	H2A-STT	8	Mg^{2+}	4 – 28
		8	$CoHex^{3+}$	1.2 – 4
7	gH2A	8	Mg^{2+}	15 – 30
		8	$CoHex^{3+}$	1.5 – 3
8	gH2B	8	Mg^{2+}	10 – 30
		8	$CoHex^{3+}$	1.5 – 5
9	gH3	8	Mg^{2+}	15 – 30
		8	$CoHex^{3+}$	1.5, 2

10	gH4	8	Mg^{2+}	15 – 30
		8	$CoHex^{3+}$	1.5 – 3
11	gH2AgH2B	8	Mg^{2+}	10 – 30
		8	$CoHex^{3+}$	1.5 – 10
12	gH3gH4	8	Mg^{2+}	10 – 30
		8	$CoHex^{3+}$	1.5 – 5
13	gH2AgH3gH4	8	Mg^{2+}	10 – 30
		8	$CoHex^{3+}$	1.5 – 5
14	gH2AgH2BgH3	8	Mg^{2+}	10 – 30
		8	$CoHex^{3+}$	1.5 – 5
15	gNCP	8	Mg^{2+}	12 – 100
		8	$CoHex^{3+}$	1.5 – 27

Abbreviations: **WT**, wild type; H4-K16Q, NCP with K→Q mutation at Lys16 of the H4 histone; **H4-K16Ac**, NCP with acetylated Lys16 of the H4 histone; **H4-QuadQ**, NCP with K→Q mutations at positions Lys5, Lys8, Lys12, Lys16 of the H4 histone; **H4-QuadAc**, NCP with acetylated Lys5, Lys8, Lys12, Lys16 of the H4 histone; **H2A-STT**, NCP with mutations D90S+E91T+E92T in the H2A histone (these 3 mutations significantly reduced negative charge of the acidic patch on the surface of histone octamer which is important for nucleosome-nucleosome interactions) ; **gH2A**, histone octamer with globular **H2A** histone (a.a. at positions 1-12 and 119-129 were truncated); **gH2B**, histone octamer with tailless H2B histone (a.a. at positions 1-21 were truncated); **gH3**, a.a. at positions 1-26) of the H3 histone were removed; **gH4**, a.a. at positions 1-19) of the H4 histone were removed; **gH2AgH2B**, NCP with tailless H2A and H2B histones; **gH3gH4**, NCP with tailless H3 and H4 histones; **gH2AgH3gH4**, NCP with tailless H2A, H3 and H4 histones; **gH2AhH2BgH3**, NCP with tailless H2A, H2B and H3 histones; **gNCP**, NCP with all four histones being tailless

Supporting Results

Collection of SAXS spectra

Figures S1 – S22 present SAXS spectra measured for all types of NCP at various concentrations of cations with most of the data obtained for the NCP samples aggregated by addition of Mg^{2+} and $CoHex^{3+}$.

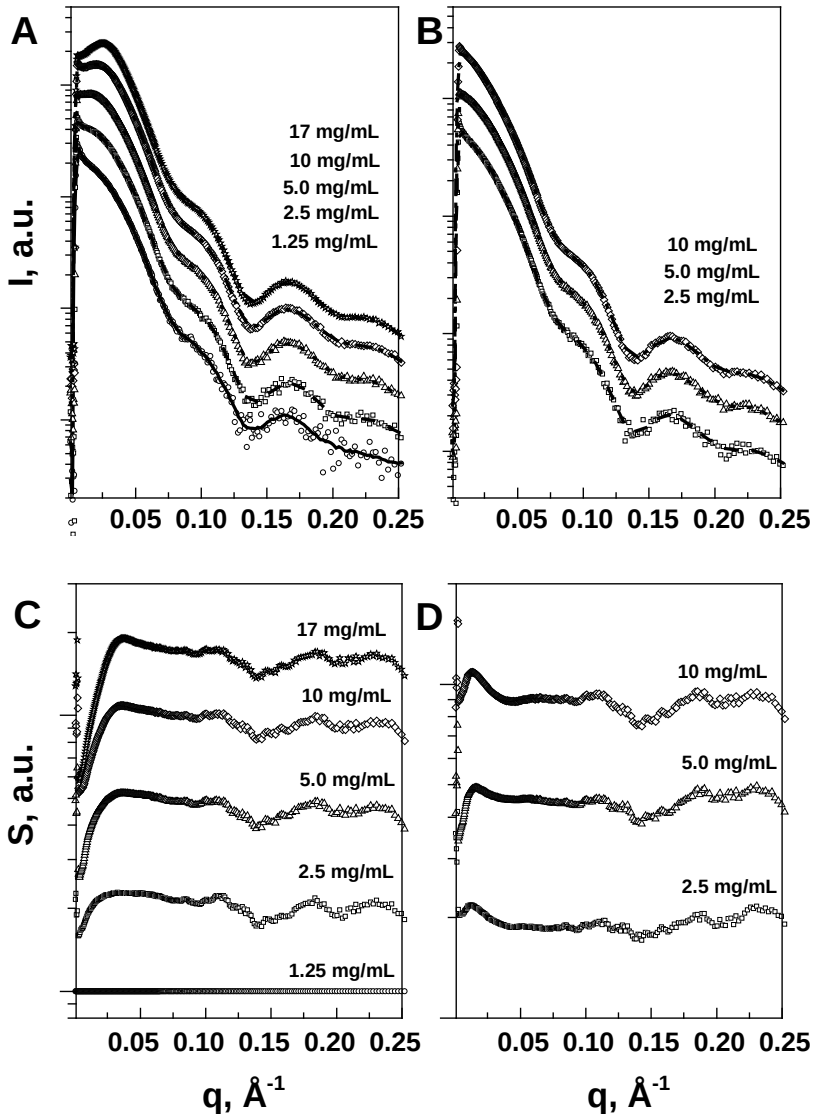

FIGURE S1. SAXS spectra (**A,B**) and calculated structure factors, S, (**C,D**) of the solutions of wild type (WT) NCP in 10 mM (**A,C**) and 100 mM (**B,D**) KCl. Concentration of the NCP in solution varied from 1.25 to 17 mg/mL (**A,C**) and from 2.5 to 10 mg/mL (**B,D**) (from bottom to top, indicated in the graphs). In **A** and **B** points are experimental data lines are 10-point averaged smoothing. Structure factors (C,D) were calculated by dividing corresponding SAXS spectra by spectrum obtained for 1.25 mg/mL solution of NCP in 10 mM KCl (i.e. under the conditions of weak and repulsive NCP-NCP interaction).

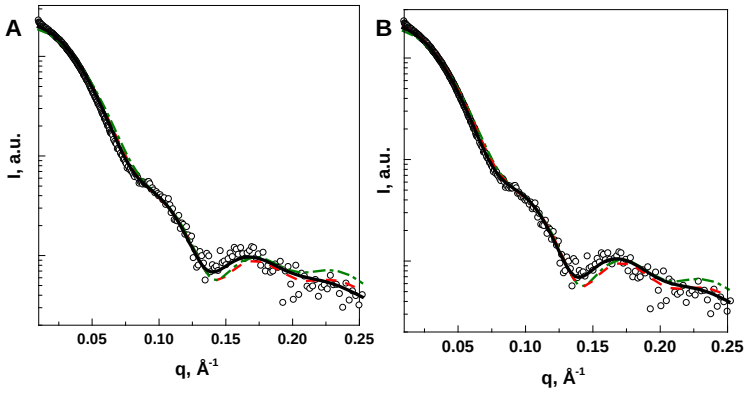

FIGURE S2. Comparison of the experimental and calculated SAXS spectra of the WT-NCP. Experimental data is for 145 bp '601' WT-NCP solution (1.25 mg/mL, 10 mM KCl). Theoretical curves were calculated using (**A**) CRYSOL software (10) or (**B**) FoXS web server (11) from three variants of the 1KX5 NCP crystal structure (8). In (**A**) and (**B**) points are experimental data; lines are results of calculations using different variants of the 1KX5 structure: (black solid line) coordinates according to the MD simulations of isolated NCP (12) with tails collapsed on the DNA and globular histone core; (red dashed line) structure as in the NCP crystal; (green dot-dashed line) tail coordinates were removed from the pdb file

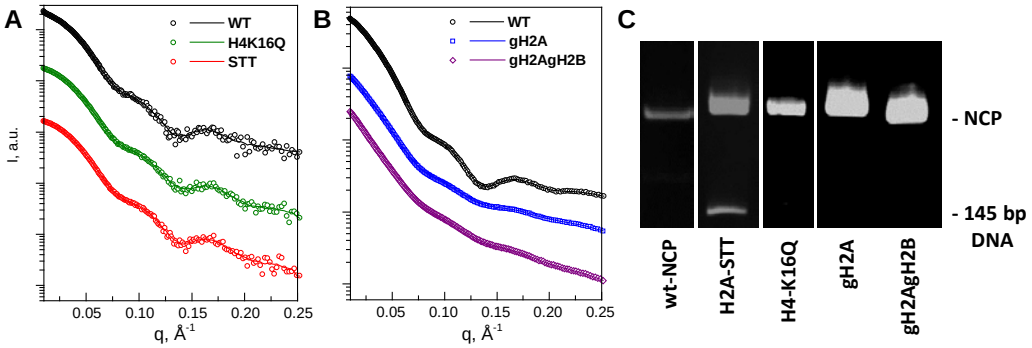

FIGURE S3. (**A**) and (**B**). Comparison of the SAXS solution spectra obtained (**A**) for WT, H4-K16Q and H2A-STT NCPs at 1.25 mg/mL concentration of NCP in 10 mM KCl; for (**B**) WT, gH2A and gH2AgH2B at 10 mg/mL concentration of NCP in 100 mM KCl. Points are experimental readings, curves are 10-point smoothing of the data. (**C**). 5% PAGE analysis of the NCP reconstitutions. Type of the NCP indicated in the figure.

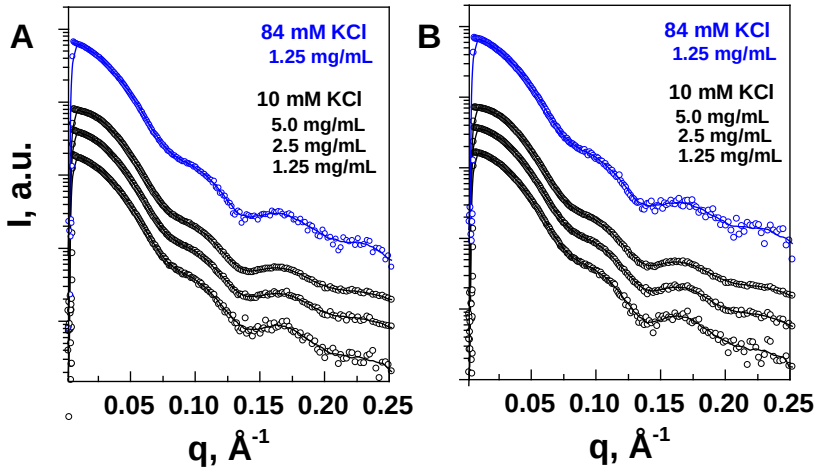

FIGURE S4. SAXS spectra of the solutions of H4-K16Q (**A**) and H2A-STT (**B**) NCPs. Concentration of the NCP in 84 mM KCl was equal to 1.25 mg/mL (blue points and curves) or was varied from 1.25 to 5 mg/mL in 10 mM KCl (black points and curves) (indicated in the graphs). Points are experimental data lines are 10 point averaged smoothing.

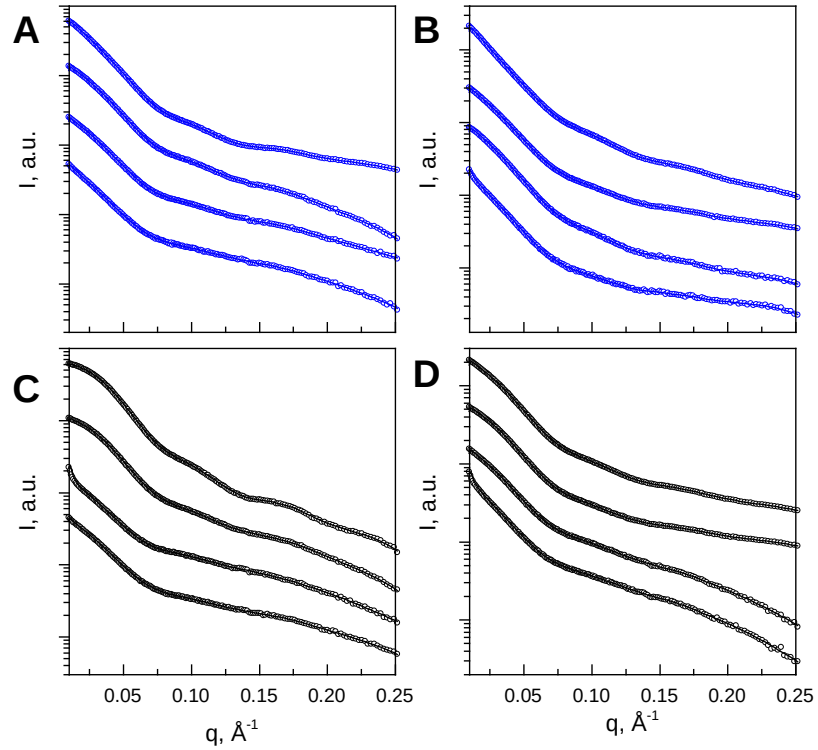

FIGURE S5. SAXS spectra of the solutions of gH2A (**A,C**) and gH2AgH2B (**B,D**) NCPs recorded in (A, B) 100 mM (blue points and curves) and (C, D) 10 mM KCl (black points and curves). In all graphs, NCP concentrations are equal 1.25, 2.5, 5.0 and 10.0 mg/mL and increase from bottom to top. Points are experimental data lines are 10 point averaged smoothing.

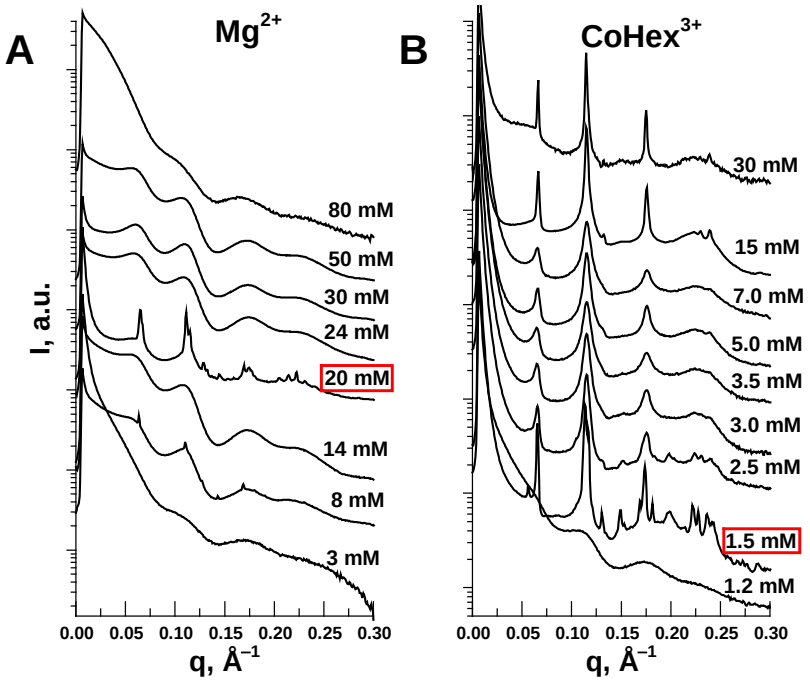

FIGURE S6. SAXS spectra of the wild type (WT) NCP in the presence of various concentrations of Mg^{2+} (**A**) and cobalt(III)hexammine^{3+} ($CoHex^{3+}$; **B**). Cation concentrations are indicated on the graphs with concentration of the most organized NCP phase highlighted by red box.

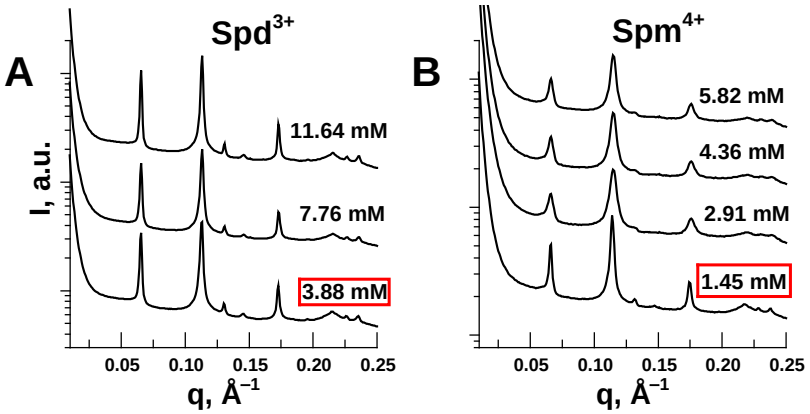

FIGURE S7. SAXS spectra the wild type (WT) NCP in the presence of various concentrations of spermidine^{3+} (Spd^{3+}; **A**) and spermine^{4+} (Spm^{4+}; **B**). Cation concentrations are indicated on the graphs with concentration of the most organized NCP phase highlighted by red box.

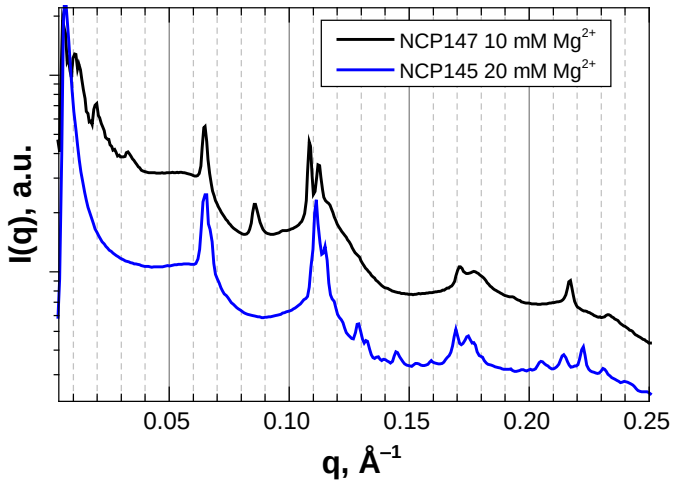

FIGURE S8. Comparison of the SAXS spectra of the two NCP samples aggregated by Mg^{2+} with different DNA templates. NCP147 (black line, top spectrum) was reconstituted on 147 bp α-satellite human DNA sequence (13); NCP145 (blue line, bottom spectrum) was prepared from the 145 bp Widom high affinity '601' DNA (6).

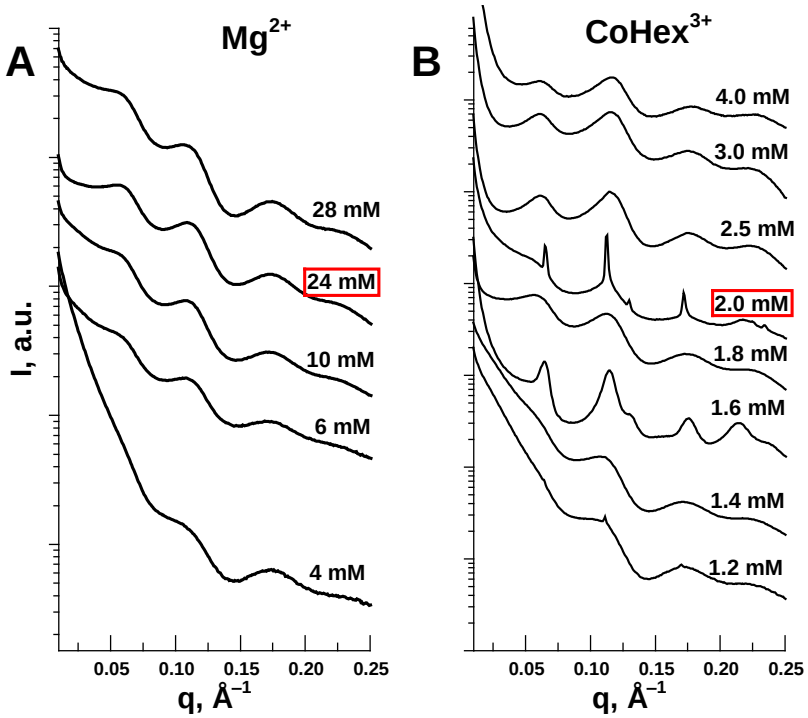

FIGURE S9. SAXS spectra of the NCP containing STT mutation of the H2A histone (D90S+E91T+E92T) in the presence of various concentrations of Mg^{2+} (**A**) and $CoHex^{3+}$ (**B**). Cation concentrations are indicated on the graphs with concentration of the most organized NCP phase highlighted by red box.

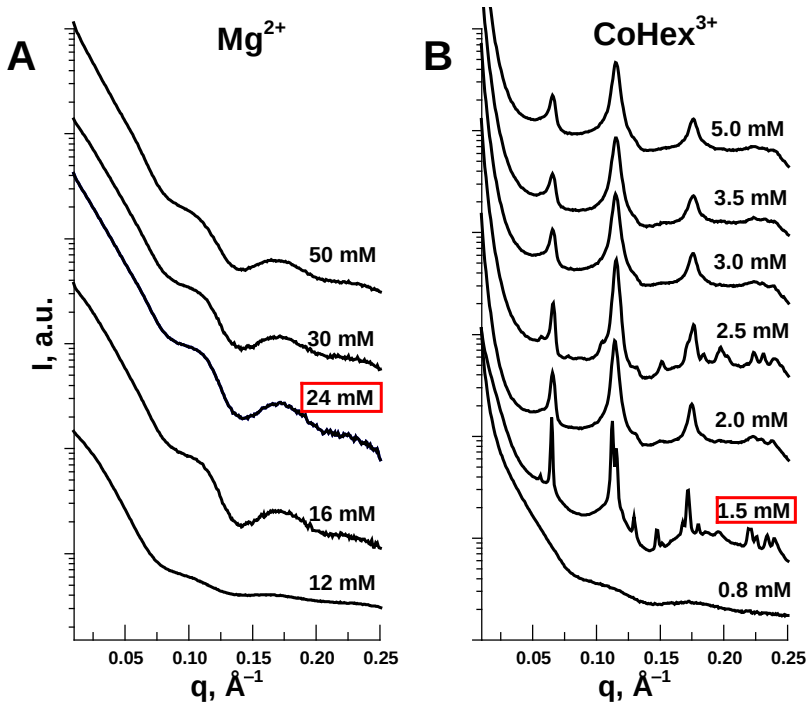

FIGURE S10. SAXS spectra of the NCP containing K16Q mutation of the H4 histone (H4-K16Q) in the presence of various concentrations of Mg^{2+} (**A**) and $CoHex^{3+}$ (**B**). Cation concentrations are indicated on the graphs with concentration of the most organized NCP phase highlighted by red box.

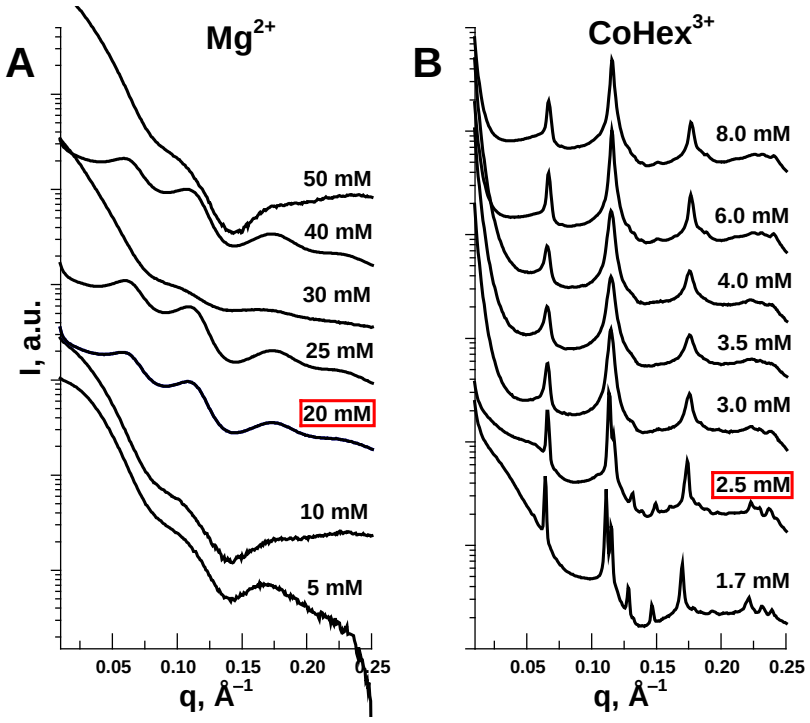

FIGURE S11. SAXS spectra of the NCP containing acetylated Lys16 in the H4 histone (H4-K16Ac) in the presence of various concentrations of Mg^{2+} (**A**) and $CoHex^{3+}$ (**B**). Cation concentrations are indicated on the graphs with concentration of the most organized NCP phase highlighted by red box.

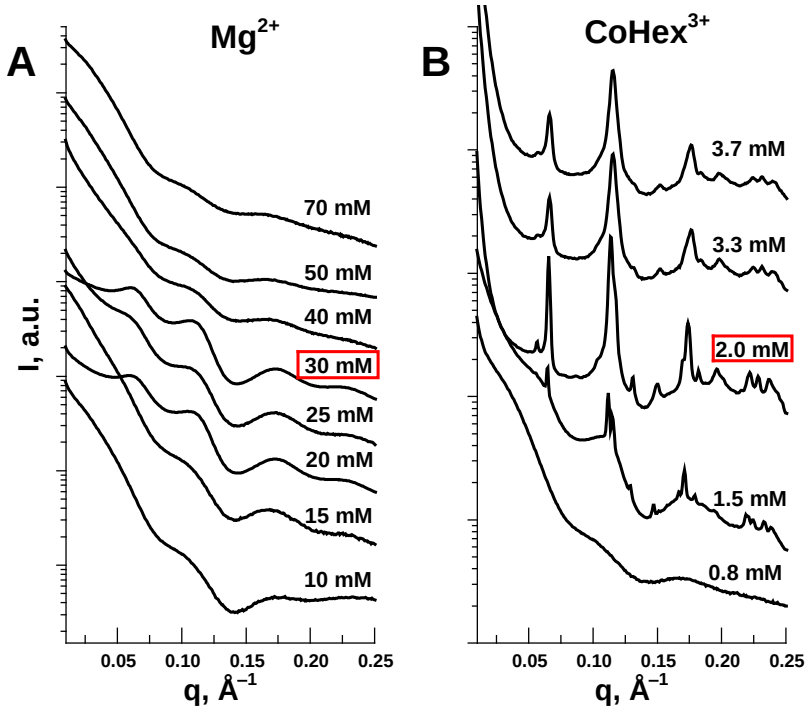

FIGURE S12. SAXS spectra of the NCP containing K5Q, K8Q, K12Q, K16Q mutations of the H4 histone (H4-QuadQ) in the presence of various concentrations of Mg^{2+} (**A**) and $CoHex^{3+}$ (**B**). Cation concentrations are indicated on the graphs with concentration of the most organized NCP phase highlighted by red box.

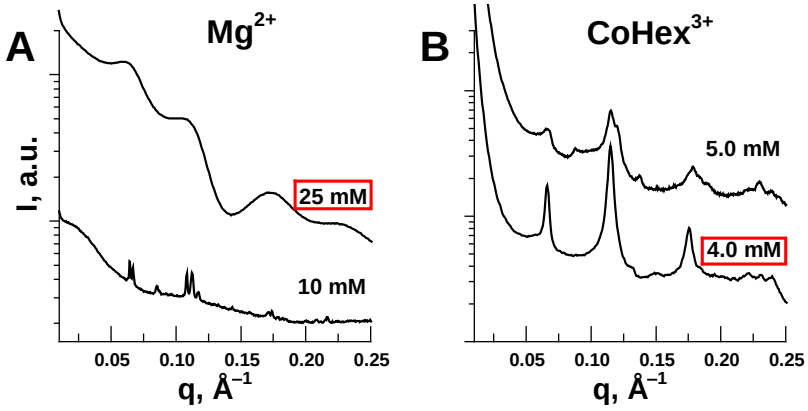

FIGURE S13. SAXS spectra of the NCP containing acetylated Lys5, Lys8, Lys12, Lys16 in the H4 histone (H4-QuadAc) in the presence of various concentrations of Mg^{2+} (**A**) and $CoHex^{3+}$ (**B**). Cation concentrations are indicated on the graphs with concentration of the most organized NCP phase highlighted by red box. Spectra at 10 mM Mg^{2+} and 5 mM $CoHex^{3+}$ were obtained with NCP containing 147 bp α-satellite human DNA sequence.

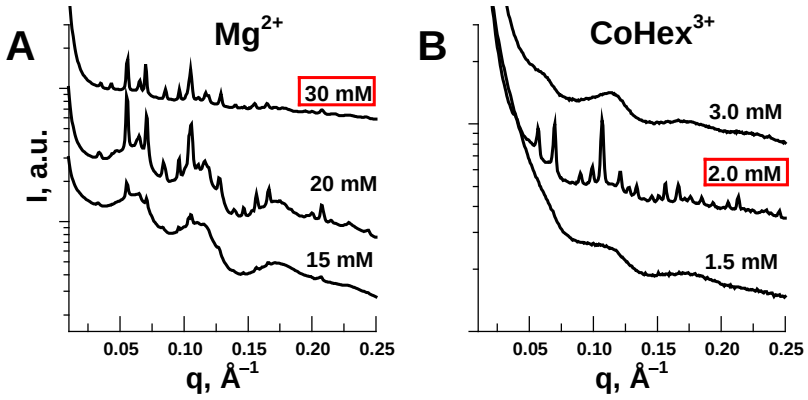

FIGURE S14. SAXS spectra of the NCP containing tailless histone H2A (gH2A) in the presence of various concentrations of Mg^{2+} (**A**) and $CoHex^{3+}$ (**B**). Cation concentrations are indicated on the graphs with concentration of the most organized NCP phase highlighted by red box.

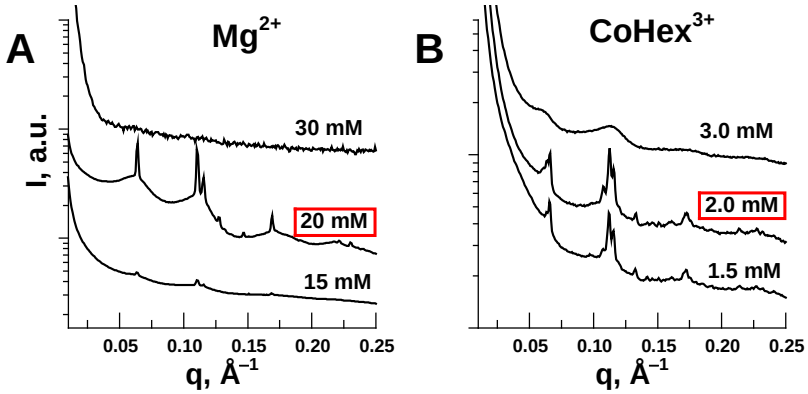

FIGURE S15. SAXS spectra of the NCP containing tailless histone H4 (gH4) in the presence of various concentrations of Mg^{2+} (**A**) and $CoHex^{3+}$ (**B**). Cation concentrations are indicated on the graphs with concentration of the most organized NCP phase highlighted by red box.

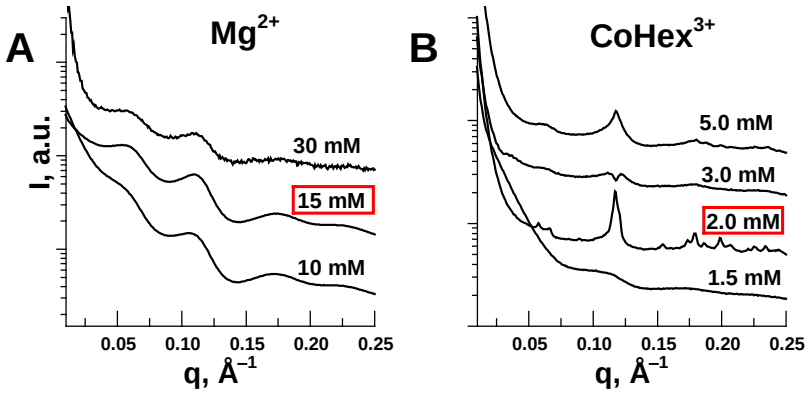

FIGURE S16. SAXS spectra (**A,B**) and calculated structure factors (**C,D**) of the NCP containing tailless histone H2B (gH2B) in the presence of various concentrations of Mg^{2+} (**A,C**) and $CoHex^{3+}$ (**B,D**). Cation concentrations are indicated on the graphs with concentration of the most organized NCP phase highlighted by red box.

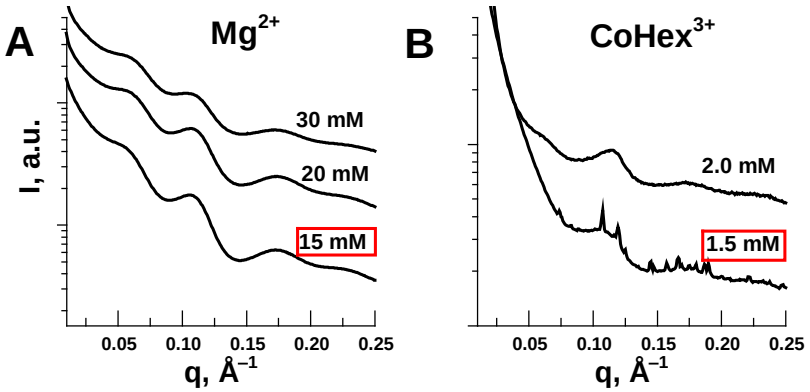

FIGURE S17. SAXS spectra of the NCP containing tailless histone H3 (gH3) in the presence of various concentrations of Mg^{2+} (A) and $CoHex^{3+}$ (**B**). Cation concentrations are indicated on the graphs with concentration of the most organized NCP phase highlighted by red box.

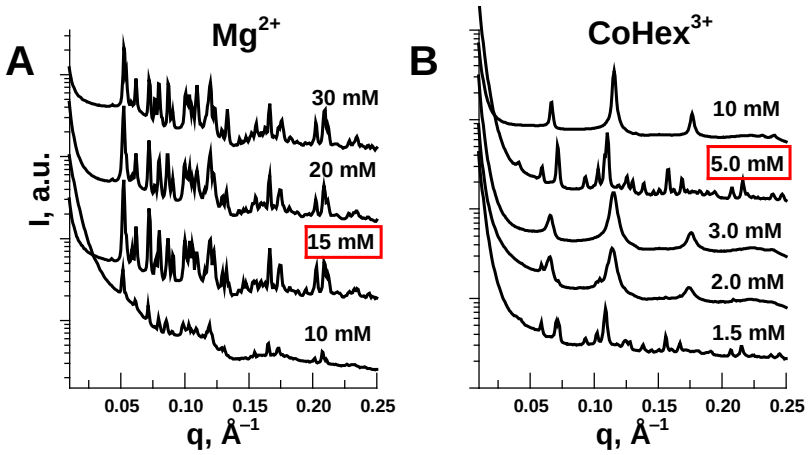

FIGURE S18. SAXS spectra of the NCP containing tailless histones H2A and H2B (gH2AgH2B) in the presence of various concentrations of Mg^{2+} (**A**) and $CoHex^{3+}$ (**B**). Cation concentrations are indicated on the graphs with concentration of the most organized NCP phase highlighted by red box.

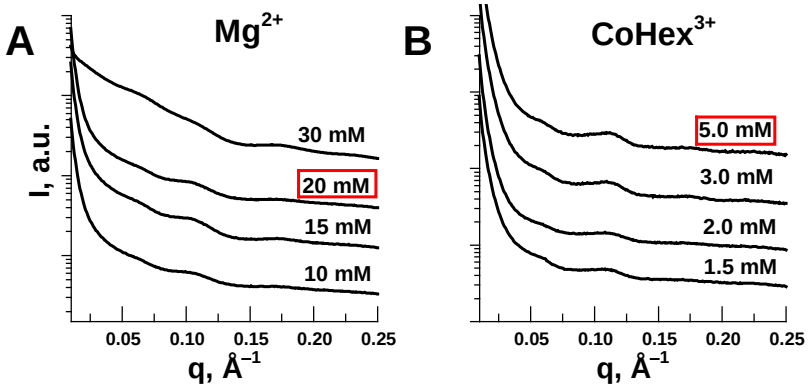

FIGURE S19. SAXS spectra of the NCP containing tailless histones H3 and H4 (gH3gH4) in the presence of various concentrations of Mg^{2+} (**A**) and $CoHex^{3+}$ (**B**). Cation concentrations are indicated on the graphs with concentration of the most organized NCP phase highlighted by red box.

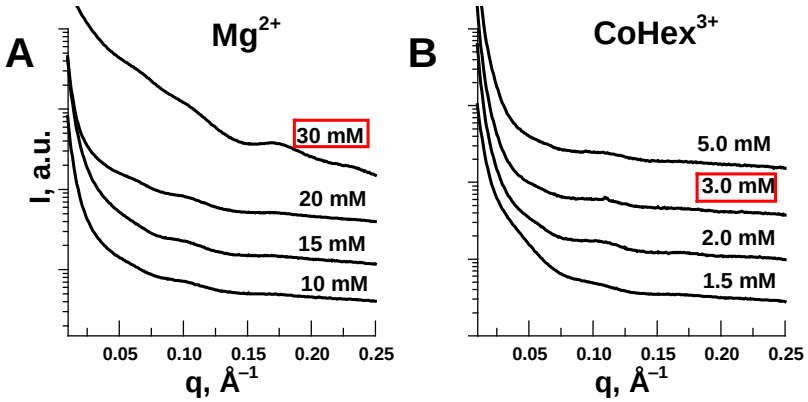

FIGURE S20. SAXS spectra of the NCP containing tailless histones H2A, H3 and H4 (gH2AgH3gH4) in the presence of various concentrations of Mg^{2+} (**A**) and $CoHex^{3+}$ (**B**). Cation concentrations are indicated on the graphs with concentration of the most organized NCP phase highlighted by red box.

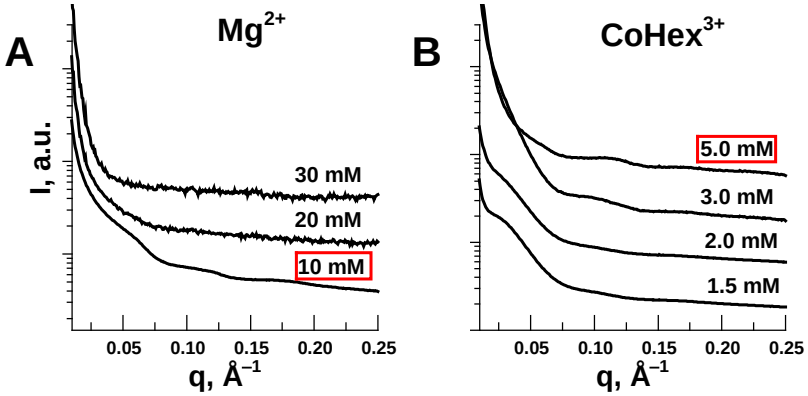

FIGURE S21. SAXS spectra of the NCP containing tailless histones H2A, H2B and H3 (gH2AgH2BgH3) in the presence of various concentrations of Mg^{2+} (**A**) and $CoHex^{3+}$ (**B**). Cation concentrations are indicated on the graphs with concentration of the most organized NCP phase highlighted by red box.

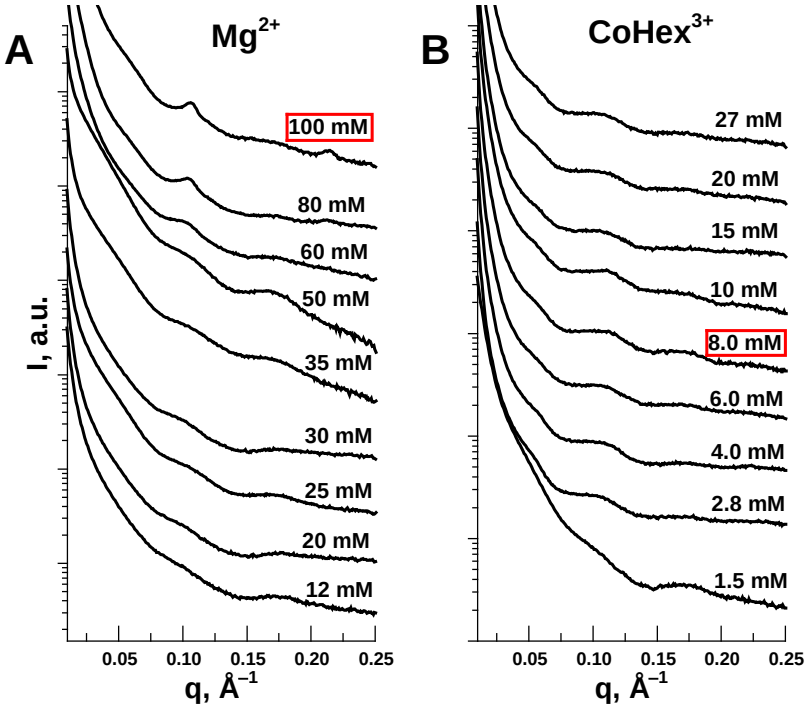

FIGURE S22. SAXS spectra of the NCP containing tailless histones (gNCP) in the presence of various concentrations of Mg^{2+} (**A**) and $CoHex^{3+}$ (**B**). Cation concentrations are indicated in the graphs with concentration of the most organized NCP phase highlighted by red box.

Table S2. Characteristic peak positions and the derived structure parameters a_H and h. SAXS spectra of the gH2A and gH2AgH2B samples are not included since for these samples structure of ordered phase is not known that prevents reliable interpretation of the peaks.

Sample	Cation	Concen-tration, mM	q_1	$q_2=\sqrt{3}\,q_1$	$q_3=\sqrt{4}\,q_1$	$q_4=\sqrt{7}\,q_1$	q_{1h}	$q_{2h}=2\,q_{1h}$	a_H (Å)	h (Å)	Phase
WT-NCP	Mg^{2+}	20 mM	0.065	0.115	0.128	0.170	0.111	0.222	111.6	56.5	3D orthorhombic
	$CoHex^{3+}$	1.5 mM	0.065	0.117	0.13	0.174	0.114	0.228	110.9	55.3	3D orthorhombic
	Spd^{3+}	3.88 mM	0.065	0.113	0.131	0.173	0.113	0.226	111.5	55.7	2D hexagonal
	Spm^{4+}	1.45 mM	0.066	0.114	0.132	0.174	0.114	0.228	110.3	55.1	2D hexagonal
H4K16Q	Mg^{2+}	24 mM									NCP isotropic
	$CoHex^{3+}$	1.5 mM	0.065	0.116	0.13	0.172	0.112	0.225	111.8	55.9	3D orthorhombic
H4K16Ac	Mg^{2+}	20 mM									NCP columnar
	$CoHex^{3+}$	2.5 mM	0.066	0.117	0.131	0.174	0.114	0.227	110.1	55.4	3D orthorhombic
H4-QuadQ	Mg^{2+}	30 mM									NCP columnar
	$CoHex^{3+}$	2.0 mM	0.066	0.117	0.131	0.174	0.114	0.228	110.7	55.2	3D orthorhombic
H4-QuadAc	Mg^{2+}	25 mM									NCP columnar
	$CoHex^{3+}$	4 mM	0.066	-*	0.132	0.175	0.115	0.231	109.9	54.6	2D hexagonal
H2A-STT	Mg^{2+}	24 mM									NCP columnar
	$CoHex^{3+}$	2.0 mM	0.065	-*	0.130	0.172	0.112	0.224	111.1	55.9	2D hexagonal
gH4	Mg^{2+}	20 mM	0.064	0.115	0.127	0.169	0.111	0.22	113.9	56.8	2D hexagonal
	$CoHex^{3+}$	2.0 mM	0.066	0.116	0.133	0.172	0.112	0.224	109.9	55.9	3D orthorhombic

gH2B	Mg^{2+}	15 mM									NCP columnar
	$CoHex^{3+}$	2.0 mM	0.066	0.117	-	0.173			110.8		3D orthorhombic
gH3	Mg^{2+}	15 mM									NCP columnar
	$CoHex^{3+}$	1.5 mM									unknown
gH3gH4	Mg^{2+}	20 mM									NCP isotropic
	$CoHex^{3+}$	5.0 mM									NCP isotropic
gH2AgH3gH4	Mg^{2+}	30 mM									NCP isotropic
	$CoHex^{3+}$	3.0 mM					0.11			57.1	NCP isotropic
gH2AgH2BgH3	Mg^{2+}	10 mM									NCP isotropic
	$CoHex^{3+}$	5.0 mM									NCP isotropic
g-NCP	Mg^{2+}	100 mM					0.106	0.214		59.4	NCP isotropic
	$CoHex^{3+}$	8.0 mM									NCP isotropic

*The first order NCP stacking peak is merged with the second order hexagonal-phase peak, and the accurate peak position cannot be determined;

- Data not available

Table S3. The domain size was estimated from the full width at half maximum (fwhm) of the first diffraction peaks in columnar hexagonal phases for the most ordered samples from Fig. 4 of the main text.

Sample	Cation	q_1					q_{1h}				
		Position	fwhm	a_H, Å	$s(a_H)$, nm	Columns	Position	fwhm	h, Å	s(h), nm	Stacked NCP
WT-NCP	Mg^{2+}	0.0650	0.0027	111.62	232	21	0.111	0.0022	56.52	280	50
WT-NCP	$CoHex^{3+}$	0.0654	0.0018	110.94	349	31	0.114	0.0028	55.31	224	41
WT-NCP,	Spd^{3+}	0.0651	0.0016	111.45	383	34	0.113	0.0023	55.65	273	49
WT-NCP	Spm^{4+}	0.0658	0.0020	110.29	313	28	0.114	0.0027	55.12	237	43
H4-K16Ac	$CoHex^{3+}$	0.0659	0.0019	110.09	338	31	0.114	0.0019	55.36	338	61
H4-K16Q	$CoHex^{3+}$	0.0649	0.0013	111.79	476	43	0.112	0.0019	55.90	324	58
H4-QuadAc	$CoHex^{3+}$	0.0660	0.0038	109.93	164	15	0.115	0.0044	54.64	142	26
H4-QuadQ	$CoHex^{3+}$	0.0656	0.0018	110.67	345	31	0.114	0.0029	55.21	217	39
H2A-STT	$CoHex^{3+}$	0.0653	0.0023	111.11	269	24	0.112	0.0020	55.90	322	58
gH4	Mg^{2+}	0.0637	0.0011	113.90	556	49	0.111	0.0014	56.81	462	81
gH4	$CoHex^{3+}$	0.0660	0.0018	109.93	355	32	0.112	0.0025	55.90	255	46
gH2B	$CoHex^{3+}$	0.0655	0.0050	110.77	126	11	-	-	-	-	-

- Data not available

REFERENCES

1. Allahverdi, A., R. Yang, N. Korolev, Y. Fan, C. A. Davey, C. F. Liu, and L. Nordenskiöld. 2011. The effects of histone H4 tail acetylations on cation-induced chromatin folding and self-association. Nucleic Acids Res. 39:1680–1691
2. Dorigo, B., T. Schalch, K. Bystricky, and T. J. Richmond. 2003. Chromatin fiber folding: requirement for the histone H4 N-terminal tail. J.Mol.Biol. 327:85-96.
3. Liu, Y., C. Lu, Y. Yang, Y. Fan, R. Yang, C.-F. Liu, N. Korolev, and L. Nordenskiöld. 2011. Influence of histone tails and H4 tail acetylations on nucleosome–nucleosome interactions. J.Mol.Biol. 414:749–764.
4. Li, F., A. Allahverdi, R. Yang, B. Lua G, X. Zhang, Y. Cao, N. Korolev, L. Nordenskiöld, and C. F. Liu. 2011. A direct method for site-specific protein acetylation. Angew.Chem.Int.Ed. 50:9611 –9614.
5. Gill, S. C., and P. H. von Hippel. 1989. Calculation of protein extinction coefficients from amino acid sequence data. Anal.Biochem. 182:319-326.
6. Lowary, P. T., and J. Widom. 1998. New DNA sequence rules for high affinity binding to histone octamer and sequence-directed nucleosome positioning. J.Mol.Biol. 276:19-42.
7. Luger, K., A. W. Mader, R. K. Richmond, D. F. Sargent, and T. J. Richmond. 1997. Crystal structure of the nucleosome core particle at 2.8 Å resolution. Nature 389:251-260.
8. Davey, C. A., D. F. Sargent, K. Luger, A. W. Maeder, and T. J. Richmond. 2002. Solvent mediated interactions in the structure of nucleosome core particle at 1.9 Å resolution. J.Mol.Biol. 319:1097-1113.
9. Jeng, U.-S., C. H. Su, C.-J. Su, K.-F. Liao, W.-T. Chuang, Y.-H. Lai, J.-W. Chang, Y.-J. Chen, Y.-S. Huang, M.-T. Lee, K.-L. Yu, J.-M. Lin, D.-G. Liu, C.-F. Chang, C.-Y. Liu, C.-H. Changa, and K. S. Liang. 2010. A small/wide-angle X-ray scattering instrument for structural characterization of air–liquid interfaces, thin films and bulk specimens. J.Appl.Cryst. 43:110-121.
10. Svergun, D. I., C. Barberato, and M. H. J. Koch. 1995. CRYSOL - a program to evaluate X-ray solution scattering of biological macromolecules from atomic coordinates. J. Appl. Cryst. 28:768-773.
11. Schneidman-Duhovny, D., M. Hammel, and A. Sali. 2010. FoXS: a web server for rapid computation and fitting of SAXS profiles. Nucleic Acids Res. 38:W540-W544.
12. Roccatano, D., A. Barthel, and M. Zacharias. 2007. Structural flexibility of the nucleosome core particle at atomic resolution studied by molecular dynamics simulation. Biopolymers 85:407-421.
13. Luger, K., T. J. Rechsteiner, and T. J. Richmond. 1999. Preparation of nucleosome core particle from recombinant histones. Methods Enzymol. 304:3-19.